

Icing Characteristics and Anti-icing Research of Supercooled Large Droplet Impact on Epoxy Composite Surfaces

LI Xiaofei^{1,2}, WANG Xiangzhao¹, JI Zemin¹, HUANG Xiaobin^{1*}, LIU Hong^{1*}

1. School of Aeronautics and Astronautics, Shanghai Jiao Tong University, Shanghai 200240, P.R.China;

2. Chinese Aeronautical Establishment, Beijing 100012, P.R.China

(Received 10 December 2024; revised 15 February 2025; accepted 20 March 2025)

Abstract: The icing characteristics of supercooled large droplet (SLD) impacting carbon fiber-reinforced composites (CFRCs) remain poorly understood, hindering the enhancement of ice protection capabilities and the certification of ice-accreted composite aircraft. The paper systematically investigates the effects of the supercooling degree, the surface temperature, and the impact velocity on the ice accretion behavior of SLDs impacting carbon fiber-reinforced epoxy composite surfaces. To address the ice-prone nature of CFRCs, nanoparticle-modified anti-icing coatings are developed, and the icing characteristics of SLD-impacted modified carbon fiber-reinforced epoxy composite surfaces are analyzed. Results demonstrate that surface-modified carbon fiber-reinforced epoxy composite exhibits significantly delayed ice formation. Under conditions of droplet temperature ($-15\text{ }^{\circ}\text{C}$) and surface temperature ($-18\text{ }^{\circ}\text{C}$), the icing time of hydrophobic-modified CFRCs was delayed by over 1 100 ms, representing a 5.4-fold improvement compared to the unmodified carbon fiber-reinforced epoxy composite.

Key words: aircraft icing; carbon fiber-reinforced epoxy composites; supercooled large droplets; hydrophobic modification; icing protection

CLC number: V321.229

Document code: A

Article ID: 1005-1120(2025)02-0178-13

0 Introduction

Carbon fiber-reinforced polymer matrix composites have been extensively utilized in structural components of rockets, missiles, aircraft, and satellites due to two distinctive advantages^[1-3]. Their design flexibility achieved through fiber orientation, layering, and stacking optimization has improved structural efficiency, while reducing weight and energy consumption, and enhancing fuel efficiency. The material system also offers high specific strength/modulus, fatigue-vibration resistance, and environmental stability. Since their adoption in military aircraft wings and empennages, these composite materials have progressively replaced metal materials in modern airframes, including Boeing 787/777, Airbus A350/A380, and Russia's MC-21^[4-5].

Notably, China's CR929 prototype demonstrates the leading composite integration, with carbon fiber/epoxy constituting 51% of its airframe weight via wing/fuselage applications^[6]. The expanding application of carbon fiber/epoxy composites in aerospace vehicles represents an irreversible technological trend, consequently driving sustained research attention toward related material advancements.

When carbon fiber-reinforced epoxy resin is utilized as wing material, ice accretion becomes an inevitable challenge, increasing surface roughness, altering the aircraft's aerodynamic configuration, and thereby modifying the surrounding flow field. These changes lead to elevated drag, reduced lift, altered stall characteristics, diminished stability/controllability, and even catastrophic accidents^[7-9]. A notable example is the Roselawn crash in 1994 involving an

*Corresponding authors, E-mail addresses: xbhuang@sjtu.edu.cn; hongliu@sjtu.edu.cn.

How to cite this article: LI Xiaofei, WANG Xiangzhao, JI Zemin, et al. Icing characteristics and anti-icing research of supercooled large droplet impact on epoxy composite surfaces[J]. Transactions of Nanjing University of Aeronautics and Astronautics, 2025, 42(2): 178-190.

<http://dx.doi.org/10.16356/j.1005-1120.2025.02.003>

ATR-72-202 aircraft operated by American Eagle Airlines, where ice-induced loss of control caused the fatal accident^[10]. The accident investigation revealed that the aircraft encountered abnormal icing caused by supercooled large droplets (SLDs), which form when ice crystals in cold air melt upon encountering warmer air. The merging of these droplets differing in size and cloud descent velocity produces larger droplets exceeding 50 μm in diameter. SLD-induced ice accretion is characterized by rapid formation, extensive coverage, and severe operational consequences^[11-15]. Multiple SLD-related crashes have compelled revisions to aviation certification standards. In response, the Federal Aviation Administration (FAA) and European Aviation Safety Agency (EASA) have amended aircraft icing airworthiness regulations, significantly enhancing requirements for ice protection systems to address SLD conditions^[16].

Recent years have witnessed growing research interest in SLD^[17-18]. Studies reveal that SLD ice accretion correlates with surface properties of impacted substrates. Wang et al.^[19] investigated SLD impingement dynamics relative to surface roughness, demonstrating increases in splashed droplet diameter, velocity, ejection angle, splash height, and mass loss rate with elevated roughness. Kong et al.^[20] explored the impact and freezing of SLD with varying supercooling degrees on inclined surfaces of differing wettability. Despite theoretical advancements, no surface property-based anti-icing strategy has been established for SLD conditions, representing a critical research gap. Current aircraft ice protection predominantly relies on active anti-/de-icing technologies such as electrothermal and hot-air systems^[21-24], which exhibit limitations including high energy consumption, restricted applicability, dependency on auxiliary infrastructure, and necessity for high thermal conductivity materials. For carbon fiber/epoxy composite wings, two intrinsic challenges arise. First, epoxy resins are inherently hydrophilic with water contact angles below 90° ^[25], promoting surface wetting and ice accumulation. Second, their low thermal conductivity (0.5—3.2 $\text{W}/(\text{m}\cdot\text{K})$) contrasts sharply with metallic alloys (e.g.,

about 150 $\text{W}/(\text{m}\cdot\text{K})$ for aluminum)^[26-27], drastically reducing thermal efficiency in active anti-icing systems. In contrast, icephobic surface engineering offers advantages including minimal energy demand, avoidance of additional weight, environmental sustainability^[28-30], and compatibility with existing protection systems to improve overall efficiency while reducing energy consumption.

Developing anti-icing surfaces for carbon fiber-reinforced epoxy composites (CFRCs) requires selecting appropriate surface engineering methods based on their icing characteristics and application requirements. Current strategies primarily focus on slippery liquid-infused porous surfaces (SLIPSs) and hydrophobic coatings. For instance, a lubricant-infused surface with metal-ion-modified substrates is fabricated in Ref. [30], achieving ice adhesion strength below 10 Pa at -48.4°C and ice formation delay time of 43 200 s at -10°C . However, the anti-icing performance of SLIPSs degrades progressively due to lubricant depletion. In contrast, hydrophobic surfaces demonstrate superior durability and environmental resistance. Zhang et al.^[31] developed a superhydrophobic epoxy coating by grafting multi-walled carbon nanotubes and silica nanoparticles, maintaining a water contact angle of 150° after 300 abrasion cycles (initial: 159°) and extending droplet freezing time by 165%. However, the synthesis process involved multi-step chemical synthesis, which was complex and not conducive to practical industrial production. Thus, creating easily manufacturable and durable passive anti-icing surfaces holds significance for enhancing composite wing performance and energy efficiency. While numerous anti-/de-icing coatings have been investigated, few studies integrate the supercooled droplet icing theory into coating design, highlighting a critical need for theory-driven surface engineering innovations.

Given existing aircraft icing protection systems and the temperature-dependent thermal conductivity of carbon fiber-reinforced composites, this paper investigates the ice accretion from SLD impingement on carbon fiber/epoxy surfaces, integrating structural and material characteristics of composites with practical demands for ice protection capabilities and

airworthiness certification requirements. Building on this foundation, the paper further explores the effects of hydrophobic surface modification on ice accretion behavior, aiming to achieve efficient anti-icing surface engineering for carbon fiber/epoxy composites. Under SLD impingement conditions, the findings provide critical technical foundations and engineering insights for developing ice-resistant surfaces in advanced composite-based aircraft wings.

1 Experiment

1.1 Materials

The carbon fiber/epoxy composite material (ZT7H/QY9611) was sourced from AVIC Composite Corporation Ltd. The ambient-cured polytetrafluoroethylene (PTFE) coating was obtained from SiFluor New Materials (Suzhou) Co., Ltd. The gas-phase nano-silica (15 nm) was acquired from Shanghai Aladdin Biochemical Technology Co., Ltd. The hydrophobic silica (15 nm) was procured from Shanghai Macklin Biochemical Technology Co., Ltd. And the polytetrafluoroethylene powder (160 nm, 95%) was supplied by Dongguan Xingwang Plastic Raw Materials Co., Ltd.

1.2 Modification method for carbon fiber/epoxy resin composites

Firstly, 20 g of ambient-cured PTFE coating dispersion was mixed with 2 g of nano-fillers (polytetrafluoroethylene powder, hydrophobic silica, or gas-phase silica) under continuous stirring for 30 min. Subsequently, the mixture was subjected to ultrasonic treatment for 30 min. Then the resulting homogeneous dispersion liquid was sprayed onto defect-free surfaces via atomized spraying with multiple passes. Finally, the coated samples were cured under ambient temperature and pressure for 24 h.

1.3 SLD impact icing process

To investigate the influence of coating wettability on the supercooled large water droplet impact icing process, an experimental setup independently developed by our research group was employed under ambient pressure to simulate supercooled large water droplet impact icing, as illustrated in Fig.1.

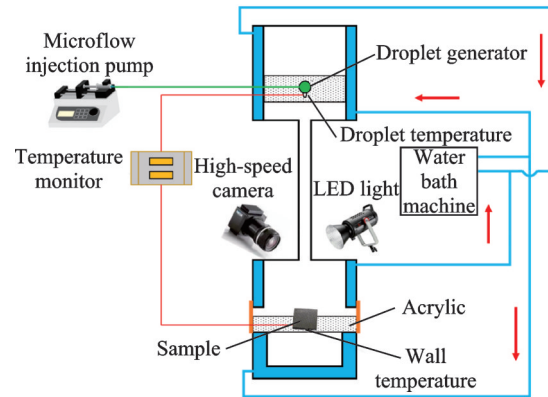


Fig.1 Schematic diagram of the SLD impact icing experimental setup

The specific experimental methodology aligns with prior publications from our group^[32-33]: All pipelines were encased in 10 mm thick insulation cotton. The upper and lower chambers are both composed of 15 mm thick acrylic resin, divided into inner and outer layers. The coolant circulation between each layer is achieved via a recirculating chiller (AP15R-30-A12Y, Polyscience, USA) to cool the entire test environment. Ultrapure water (0.97 μL) was propelled by a microfluidic syringe pump (LSP02-1B, Longer Precision Pump Co., Ltd.) through a nozzle to generate supercooled large water droplets that ultimately impact the surface of the sample placed horizontally directly beneath the nozzle. Real-time temperature monitoring of ultrapure water and samples was implemented using temperature sensors (XMT-JK808, Yutai Instrument Co., Ltd.), with thermal resistors (PT100, Heraeus) attached 5 mm below the droplet generator orifice and on sample sidewalls to measure droplet and surface temperatures. Temperature control was maintained through chiller-regulated coolant circulation. The supercooled droplet impact icing process was recorded by a high-speed camera (Phantom VEO710L, Vision Research, USA). Temperature deviations for both supercooled droplets and wall surfaces were controlled within 0.2 $^{\circ}\text{C}$. In this experiment, the droplet diameter was fixed at (2.1 ± 0.1) mm, and the impact velocity remained (2.04 ± 0.03) m/s unless otherwise specified.

1.4 Wettability characterization

To characterize the wettability of the coating,

the water contact angle was measured using a contact angle measuring instrument (JCY-4, Shanghai Fangrui Instrument Co., Ltd.) under ambient temperature and pressure. At room temperature, 5 μL of distilled water was vertically deposited onto five distinct locations of the sample, and the average value of the water contact angle was obtained.

1.5 Image measurement method

Regarding parameters such as droplet dimensions (particle size, spreading diameter, freezing diameter, etc.), the pixel analogy method is employed: An object of known dimensions is placed at the same position, and the droplet size D is obtained by

$$D = D' \frac{S}{S'} \quad (1)$$

where S denotes the number of pixels corresponding to the water droplet size, D' the actual length of the object, and S' the pixel count corresponding to the object's length.

1.6 Surface topography and roughness characterization

To characterize the surface morphology of the coating, a high-resolution field emission scanning electron microscope (Sirion 200) was employed for

observation.

To characterize the surface roughness of the coating, the Keyence VK-X3000 confocal laser scanning microscope was utilized for observation.

2 Results and Discussion

2.1 Influence of composite material surface temperature on mechanisms of SLD impact ice accretion

Generally, when materials are exposed to different ambient temperatures, their surface temperature inevitably changes. Similarly, external substances contacting surfaces at different temperatures exhibit distinct morphologies. Aircraft in flight frequently encounter icing meteorological conditions with the varying temperatures, thus making the study of wall temperature effects on SLD impact ice accretion critical for guiding anti-icing designs. This paper investigates the influence of wall temperatures (-10 , -12 , and -14 $^{\circ}\text{C}$) on SLD impact ice accretion. Fig.2 illustrates the icing process of -15 $^{\circ}\text{C}$ supercooled water impacting walls at these three temperatures. Key parameters such as ice diameter and freezing time are listed in Table 1. As shown in Fig.2, SLD droplets reach the maximum spreading

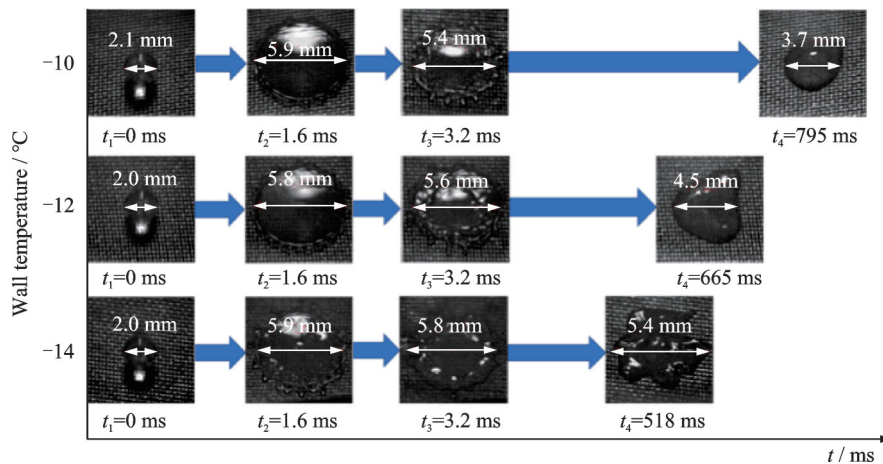


Fig.2 Freezing situation of supercooled water with temperature of -15 $^{\circ}\text{C}$ hitting different wall temperatures

Table 1 Droplet diameter and complete freezing time for different wall temperatures and impact velocities

Temperature/ $^{\circ}\text{C}$	Velocity/ $(\text{m}\cdot\text{s}^{-1})$	Maximum spreading diameter/mm	Recoiling diameter/mm	Complete freezing diameter/mm	Complete freezing time/ms
-10	2.04	5.9	5.4	3.7	795
-12	2.04	5.8	5.6	4.5	665
-14	2.04	5.9	5.8	5.4	518
-10	2.54	6.2	6.0	4.9	604
-10	3.43	6.4	6.3	5.7	420

stages at 1.6 ms post-impact, with nearly identical maximum diameters (about 5.9 mm). During subsequent retraction stages at 3.2 ms, retraction diameters increase with the decreasing wall temperature due to faster nucleation at lower temperatures, thus accelerating the ice formation. This phenomenon is more pronounced in the t_4 phase of Fig.2: Ice forms post-retraction at $-10\text{ }^\circ\text{C}$ but during retraction at $-12\text{ }^\circ\text{C}$ and $-14\text{ }^\circ\text{C}$. Although the latter two share similar icing modes, their retraction extents differ significantly. Results demonstrate that lower temperatures promote faster nucleation and smaller retraction extents. Typically, the droplet transparency progressively decreases until stabilization, indicating complete freezing.

Wall temperature significantly influences ice formation modes, thereby affecting final freezing diameters and freezing durations. As demonstrated in Fig.2 and Table 1, decreasing wall temperatures from $-10\text{ }^\circ\text{C}$ to $-14\text{ }^\circ\text{C}$ can increase freezing diameters from 3.7 mm to 5.4 mm and reduce complete freezing time from 795 ms to 518 ms. This phenomenon arises because lower wall temperatures enhance droplet nucleation rates and accelerate nucleation kinetics, promoting larger ice accretion dimen-

sions and shorter phase-change completion periods.

2.2 Effect of impact velocity on icing dynamics of SLD

To investigate the influence of SLD impact on the icing characteristics of epoxy carbon-fiber composites, this paper examines the effect of impact velocity on the SLD icing behavior on composite surfaces. Different impact velocities were adjusted by controlling the height between the droplet generator and the test specimen. To ensure the accuracy of the results, the supercooling degree and wall temperature were maintained constant at $-15\text{ }^\circ\text{C}$ and $-10\text{ }^\circ\text{C}$, respectively. The study focuses on icing processes at impact velocities of 2.04, 2.54, and 3.43 m/s, revealing the correlation between impact velocity and ice formation patterns on composite surfaces. As shown in Fig.3, significant differences exist in the time required to reach the maximum spreading diameter after droplet-wall impact under the three velocities. Specifically, the time to achieve maximum spreading diameters at 2.04, 2.54, and 3.43 m/s is 1.6, 1.4, and 1.0 ms, respectively. The observed trend demonstrates that higher impact velocities correlate with shorter time to reach maximum spreading diameters.

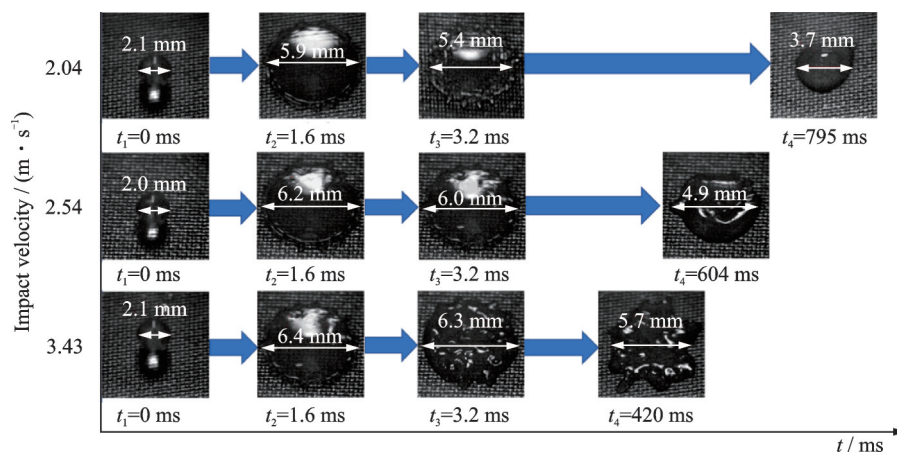


Fig.3 Icing process of SLD with different impact velocities

To better investigate the impact velocity's influence on SLD icing, this study analyzes the icing process at the same t_3 moment (3.2 ms). As shown in Fig.3, increasing impact velocity induces more ice nuclei at t_3 , which progressively restricts droplet retraction, slows the retraction rate, and ultimately

enlarges the droplet diameter during the retraction phase. Fig.3 and Table 1 demonstrate that the complete freezing diameter increases from 3.7 mm to 5.7 mm, while the complete freezing time decreases from 795 ms to 420 ms as impact velocity rises. The 3.43 m/s case exhibits only a 0.7 mm difference be-

tween complete freezing diameter and maximum spreading diameter, with negligible retraction due to earlier attainment of spreading diameter at higher velocities, which accelerates ice nucleation and suppresses retraction. The observed freezing time reduction correlates directly with the earlier ice nucleation initiation. In summary, higher impact velocities promote ice nucleation dominance over retraction dynamics, thereby accelerating phase transition and shortening freezing duration.

According to the classical nucleation theory, the nucleation rate is principally governed by the free energy barrier and temperature^[34-35], shown as

$$J = Ke^{\frac{-\Delta G}{k_B T}} \quad (2)$$

where K represents the kinetic pre-exponential factor, ΔG the nucleation free energy, k_B the Boltzmann constant, and T the system temperature. The influence of ΔG on nucleation rate substantially outweighs that of the pre-exponential factor K ^[34]. At constant temperature, the nucleation rate of supercooled water is primarily determined by the free energy barrier ΔG . Wu et al.^[36] observed that nucleation rates increased by several orders of magnitude with rising impact velocities under fixed experimental temperatures ($-14\text{ }^\circ\text{C}$), consistent with our findings, demonstrating that impact-induced perturbations significantly promote nucleation. This occurs because microscopic fluctuations in supercooled water under non-equilibrium conditions are amplified by external disturbances. When fluctuation energies exceed the nucleation barrier of supercooled water, the ice nuclei forms. The droplet-wall collision generates intense energy dissipation during impact, enhancing energy fluctuation effects, which effectively modify the energy barrier required for spontaneous nucleation in supercooled water. Specifically, higher impact velocities induce stronger disturbances, amplify fluctuation effects, reduce the required ΔG , and accelerate nucleation^[36-37].

2.3 Frozen spreading rate law of SLD

As illustrated in Figs.2, 3, the freezing diameter of SLDs impacting epoxy carbon fiber composite surfaces is related to both wall temperature and impact velocity. In other words, the freezing area is in-

trinsically linked to wall temperature and impact velocity. The above findings indicate that a smaller freezing area corresponds to the longer freezing time, consequently, investigating the variation patterns of freezing area holds significant importance. To further analyze the variation in freezing area, this study employs the average freezing spreading rates (β_{real}) to characterize the freezing features of droplet impacts, shown as

$$\beta_{\text{real}} = \frac{D_{\text{final}}}{D_{\text{max}}} \quad (3)$$

where D_{max} represents the maximum spreading diameter, and D_{final} the final frozen diameter. Experiments were conducted under five distinct supercooling degrees at the same wall temperature ($-14\text{ }^\circ\text{C}$) and impact velocity, with corresponding data obtained using the aforementioned formula. β_{real} for different supercooling degrees are shown in Fig.4. When the supercooling degree was below $10\text{ }^\circ\text{C}$, the freezing spreading rate of the epoxy carbon fiber composite exhibited relatively minor variations, with β_{real} values of 0.6 and 0.64 at supercooling degrees of $8\text{ }^\circ\text{C}$ and $10\text{ }^\circ\text{C}$, respectively. As the supercooling degree increased from $10\text{ }^\circ\text{C}$ to $12\text{ }^\circ\text{C}$, β_{real} rose significantly from 0.64 to 0.76, demonstrating a pronounced upward trend. This increasing trend persisted without attenuation as supercooling further increased, ultimately reaching 0.92. The data in Fig.4 indicate that β_{real} for the carbon fiber epoxy composite gradually approaches its theoretical maximum value of 1. This behavior differs from the spreading rate patterns observed by Sun et al.^[33] on hydrophilic aluminum surfaces (contact angle: 51.7°), instead resembling those of bare aluminum surfaces (contact angle: 91.5°). Generally, larger contact angles correlate with more pronounced increases in freezing spreading rates. However, subsequent studies revealed that the carbon fiber epoxy composite, despite having a contact angle below 90° (indicating partial hydrophilicity), exhibited spreading behavior akin to bare aluminum surfaces. This discrepancy may arise from the composite's low thermal conductivity, which reduces its temperature sensitivity compared to metals. Consequently, under identical controlled temperature conditions, the

composite's surface temperature might slightly exceed that of metallic surfaces. These experimental results demonstrate that lower supercooling degrees minimally influence freezing spreading rates, while higher supercooling degrees induce significant increases in spreading rates with rising supercooling.

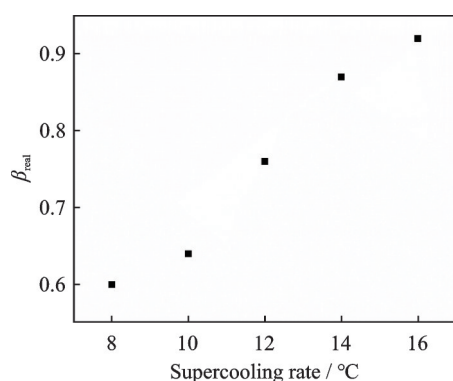


Fig.4 Frozen spreading rate of supercooled water droplets on CFRCs

2.4 Effect of surface modification on wettability of CFRCs

Previous systematic investigations on SLD impact icing processes of CFRCs revealed that, although their freezing spreading rates did not follow patterns similar to hydrophilic aluminum surfaces, their freezing time remained relatively rapid. From an anti-/de-icing perspective, the observed freezing time offer no substantial advantages for ice prevention or removal. Furthermore, the inherently high strength and rigidity of CFRCs result in significant mechanical interlocking effects between the ice and the material surface during icing, which hinders ice detachment. Consequently, to enhance the competitive edge of CFRCs as alternatives to metallic alloys, surface modification becomes imperative for optimizing their icephobic performance and interfacial adhesion characteristics.

This study selected PTFE coatings with low surface energy, low viscosity, and transparency as the matrix, since low surface energy enhances hydrophobicity, low viscosity facilitates straightforward spray application, and transparency broadens applicability. To optimize icephobic performance, three distinct fluorine/silicon-based nanoparticles were incorporated for hydrophobic modification:

PTFE particles for surface energy reduction, hydrophobically modified silica containing abundant hydrophobic functional groups, and fumed silica for constructing surface micro-nano structures. The preparation process involved first blending PTFE coatings with PTFE powder, hydrophobic silica, or fumed silica separately, then spray-coating these three mixtures onto carbon fiber epoxy resin composites, followed by curing to produce modified specimens designated as Coating 1, Coating 2, and Coating 3, as shown in Fig.5, where the magnification of the first row, the second row, and the third row are 100, 2 000, 20 000, respectively. For comparative analysis of surface modification effect and nanoparticle contributions, contact angles were measured for both unmodified carbon fiber epoxy composites and PTFE-modified counterparts (Fig.6), and complemented by surface morphology characterization and roughness quantification.

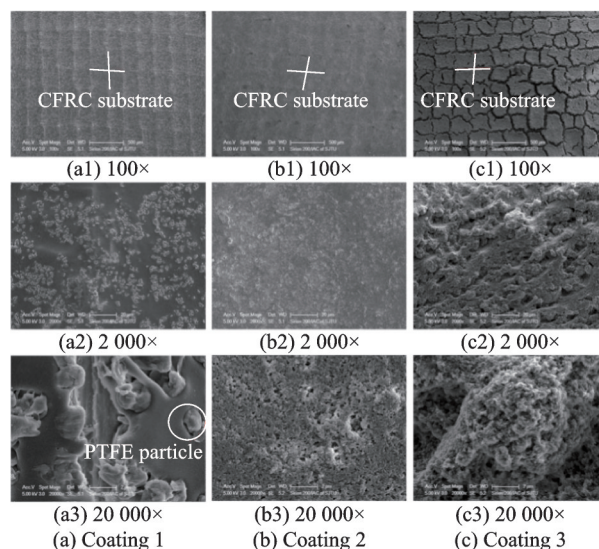


Fig.5 SEM images of different coatings

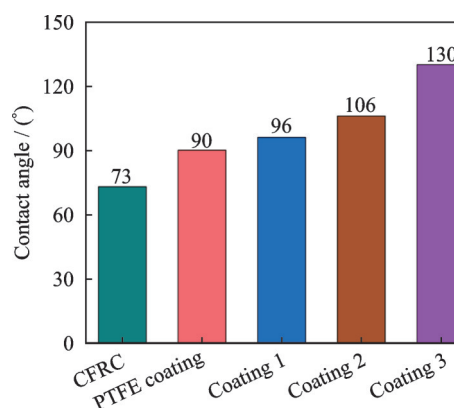


Fig.6 Contact angle of CFRCs before and after modification

The water contact angles for the PTFE coating, Coating 1, Coating 2, and Coating 3 were measured as 90° , 96° , 106° , and 130° , respectively. The incorporation of three distinct nanoparticles yielded surfaces with varying wettability, demonstrating that altering nanoparticle types alone enables tunable hydrophobic properties. To elucidate the differences in wettability among the three coatings, this study employed scanning electron microscopy (SEM) and confocal laser scanning microscopy (CLSM) for surface characterization. SEM images (Figs.6(a1, b1, c1)) revealed a distinct cross-weave structure in the carbon fiber-reinforced epoxy resin substrate, as highlighted by red lines. The polymer coatings conformed to this interlaced architecture, with Coating 3 (incorporating fumed silica) exhibiting the most pronounced surface topography (Figs.6(c1, c2)) due to its hierarchical micro-nano structures. In contrast, Coating 2 (modified with hydrophobic silica) displayed a smoother surface compared to Coatings 1 and 3, attributed to the smaller particle size and improved compatibility of hydrophobic silica with the coating matrix, which became embedded without forming complex microstructures, resulting in its moderate hydrophobicity (106°) relative to Coating 3 (130°). Although Coating 1 exhibited micron-scale textures, its PTFE particles (indicated by red circles in Fig.6(a3)) with submicron dimensions (about 100 nm) failed to generate sufficient microcavities to sustain the Cassie-Baxter state for water droplets, limiting its contact angle to 96° . Conversely, Coating 3 featured synergistic micron-scale protrusions and nanoscale asperities, enabling the formation of stable air pockets that effectively supported both static droplets and supercooled water in a metastable state, thereby achieving superior hydrophobicity.

Confocal microscopy further corroborated these observations. As shown in Fig.7, Coating 2 exhibited the smoothest surface, with protrusions measuring only $6.1 \mu\text{m}$ above the resin substrate in Fig.7(b), significantly lower than those of Coating 1 ($9.5 \mu\text{m}$) and the roughest Coating 3 ($29.5 \mu\text{m}$). Fig.7(c) illustrates that most regions of Coating 3 protruded approximately $10 \mu\text{m}$ above the sub-

strate, with fumed silica aggregation sites reaching $29.5 \mu\text{m}$. Areal roughness (S_a) measurements via confocal microscopy revealed S_a values of $1.9 \mu\text{m}$ and $1.8 \mu\text{m}$ for Coatings 1 and 2, respectively. Despite micron-scale textures in Coating 1, its large-sized PTFE particles (as shown in Fig.7) failed to achieve effective stacking for hierarchical roughness. In contrast, Coating 3 displayed a markedly higher S_a of $10.3 \mu\text{m}$, attributable to its synergistic micron-scale architectures and nanoscale asperities, which collectively enhanced surface roughness and facilitated air pocket formation to support both static droplets and impacting supercooled water. Generally, higher contact angles correlate with extended ice formation delays during SLD impacts, prompting subsequent investigations into the influence of surface modifications on SLD icing characteristics.

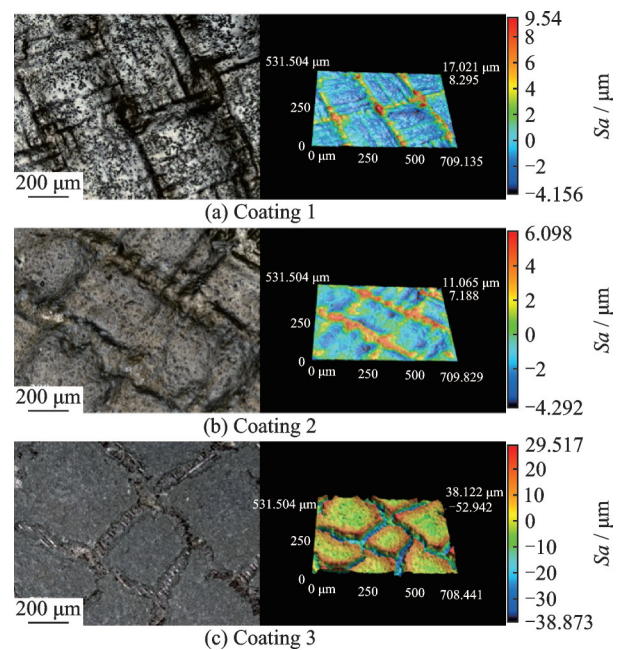


Fig.7 Confocal laser microscope images and 3D images of different coatings

2.5 Effect of surface modification on SLD impact icing characteristics

To further clarify the effects of surface modification on SLD impact icing characteristics, this study conducted investigations under controlled conditions with supercooled water at -15°C and a wall temperature of -18°C . Fig.8 illustrates the ice formation phenomena following SLD impacts on four distinct surfaces. The moment of SLD-wall contact

was defined as $t=0$. Post-impact, water droplets rapidly spread, reaching maximum spreading diameters across all four surfaces at approximately 1.6 ms, which indicates consistent maximum spreading time regardless of surface modifications when supercooling degree, impact velocity, and wall temperature remain constant.

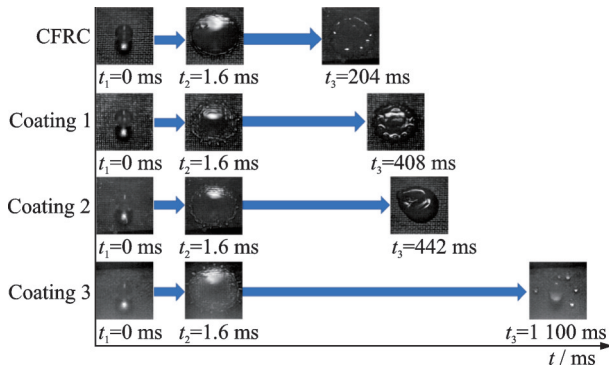


Fig.8 Freezing process of SLDs hitting walls with different wettabilities

As shown in Fig.8, the unmodified CFRC exhibited initial ice nucleation during maximum spreading, whereas none of the three hydrophobic modified surfaces displayed similar behavior. Significant differences in droplet retraction dynamics and retraction extent were observed among the four surfaces. These variations primarily correlate with interfacial contact area and heat transfer mechanisms. Among the three fundamental heat transfer modes, thermal conduction dominates at the droplet-wall interface in this system. For the unmodified composite, ice formation occurred during retraction, aligning with previous studies on wall temperature effects under supercooling degrees of 12 °C and 14 °C, where retraction-phase icing was consistently observed. However, the retraction extent decreased progressively with lower wall temperatures, demonstrating that wall temperature modulates SLD icing behavior through multiple pathways rather than inducing a singular icing mode.

The enhancement of hydrophobic angles via nanoparticles typically involves constructing rough surfaces, which significantly influence heat transfer. Generally, for rough surfaces, larger contact angles correspond to smaller contact areas between the ob-

ject and the surface, resulting in slower heat transfer. For Coatings 1 and 2, the ice formation occurred during droplet retraction, yet their retraction extents differed markedly, with Coating 2 exhibiting greater retraction. This disparity arises from the superior hydrophobicity of Coating 2, which minimizes droplet-surface contact area, slows heat transfer, and thereby prolongs ice formation time. Notably, Coating 3 demonstrated no ice formation even after 1100 ms, with the droplet nearly restoring its original shape and size. Compared to the unmodified epoxy composite, Coating 3 extended ice formation time by over 5.4-fold. This exceptional performance stems from the incorporation of fumed silica, which creates a uniformly distributed micro-nano hierarchical structure, further increasing contact angle and hydrophobicity. Consequently, Coating 3 achieves significantly reduced contact area and contact time with droplets compared to Coating 2, impeding heat absorption or dissipation from the droplet. This thermal isolation mechanism prevents ice nucleation and allows sufficient time for complete droplet retraction to its original dimensions. These findings highlight outstanding anti-icing effect of Coating 3, demonstrating strong potential for practical engineering applications.

In addition, according to the classical nucleation theory, the free energy of nucleation ΔG is expressed as^[38]

$$\Delta G = \frac{16\pi\gamma_{LX}^3 (2 + \cos\theta)(1 - \cos\theta)^2}{3\Delta G_V^2} \quad (4)$$

Herein, the water contact angle (WCA) is represented by θ , the liquid-nucleus interfacial energy by γ_{LX} and the volumetric Gibbs free energy difference by ΔG_V . A significantly positive correlation between WCA and ΔG has been established, where larger WCA corresponds to higher ΔG , thereby increasing the energy barrier for droplet nucleation. This theoretical framework confirms that enhancing coating hydrophobicity (i.e., increasing WCA) effectively prolongs droplet freezing time by elevating the nucleation energy threshold, which is fully consistent with the ice retardation phenomena observed in this study.

2.6 Effects of different wall temperatures on icing behavior of Coating 3

The study revealed that Coating 3 exhibited exceptional anti-icing performance, with no droplet freezing observed within the experimental time-frame. To further investigate its ice-resistant properties under extreme conditions, the anti-icing performance of Coating 3 was evaluated at lower wall temperatures. As shown in Fig.9, under a controlled supercooling degree of $-15\text{ }^{\circ}\text{C}$, wall temperatures were adjusted to -20 , -22 , and $-24\text{ }^{\circ}\text{C}$, respectively, and ice formation was monitored during the impact of SLDs on the coating surface. The SLD impact process distinctly comprised a spreading phase (t_2) and a retraction phase (t_3). Experimental observations demonstrated that decreasing wall temperatures progressively reduced the retraction magnitude, shortened the ice formation time, and increased the frozen area. This phenomenon arises from accelerated ice growth kinetics at lower wall temperatures, which suppresses the droplet retraction during freezing. While the ice nucleation consistently occurred during retraction across all three wall temperatures, the retraction magnitude and the resultant ice formation time differed significantly. As the wall temperature decreased from $-20\text{ }^{\circ}\text{C}$ to $-24\text{ }^{\circ}\text{C}$, the freezing time decreased from 866 ms to 288 ms. Notably, even at $-24\text{ }^{\circ}\text{C}$, the freezing time (288 ms) remained longer than that of the unmodified epoxy composite at $-18\text{ }^{\circ}\text{C}$. These results confirm that the modified CFRC retains measurable ice resistance under extreme conditions, further evidencing the outstanding anti-icing efficacy of surface modification.

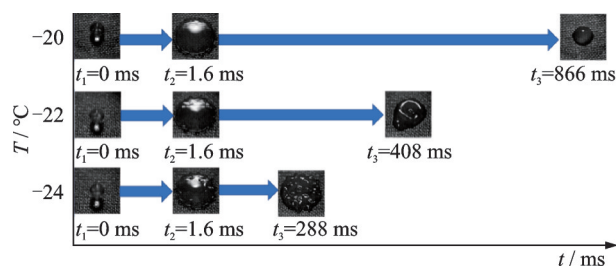


Fig.9 Freezing situation of SLDs with a temperature of $-15\text{ }^{\circ}\text{C}$ hitting different wall temperatures

3 Conclusions

This study investigated the ice formation pro-

cess of SLDs impacting CFRCs before and after surface modification through SLD impact experiments. The key conclusions are as follows:

(1) Wall temperature and droplet impact velocity significantly influence ice formation characteristics on the composite surface: Lower wall temperatures and higher impact velocities accelerate droplet nucleation, shorten the impact-induced freezing time, and reduce retraction magnitude.

(2) When droplet supercooling is below $10\text{ }^{\circ}\text{C}$, the supercooling degree exhibits negligible effects on the freezing spread rate. However, when supercooling exceeds $10\text{ }^{\circ}\text{C}$, the freezing spread rate sharply increases and progressively approaches the theoretical maximum of 1.

(3) A uniform micro-nano structured surface was constructed on the epoxy composite via a hybrid coating of fumed silica and PTFE, significantly enhancing its anti-icing performance. Under conditions of $-15\text{ }^{\circ}\text{C}$ supercooled water and $-18\text{ }^{\circ}\text{C}$ wall temperature, droplets remained unfrozen even after 1 100 ms, representing a 5.4-fold increase in freezing time compared to unmodified samples.

(4) Surface modification of CFRCs for superior anti-icing performance was achieved through a simple mixing and spraying method. This approach features operational simplicity, ease of implementation, and potential for industrial scalability, providing theoretical foundations and technical support for developing anti-icing surfaces on carbon fiber-reinforced composite aircraft wings.

References

- [1] HUANG Chunfang. High stiffness and high strength design of composite wing spar[D]. Hunan: National University of Defense Technology, 2018.(in Chinese)
- [2] ZHANG Y, ZHANG J, ZHENG Y. The thermal expansion behavior of carbon fiber-reinforced resin mineral composite postured under various temperatures[J]. Journal of Reinforced Plastics and Composites, 2017, 36(7): 505-518.
- [3] ZHOU Qi, YE Yiyun, JIAO Junke, et al. Performance analysis of carbon fiber reinforced thermal setting composite-titanium alloy laser joint[J]. Acta Aeronautica et Astronautica Sinica, 2022, 43(2): 171-184. (in Chinese)
- [4] XU Rongxia, GAO Jianxiong, ZHU Pengnian, et al. Fatigue life prediction method for fiber reinforced com-

- posite laminates[J]. *Journal of Shanghai Jiao Tong University*, 2024, 58(3): 400-410.(in Chinese)
- [5] MATHIJSSEN D. How safe are modern aircraft with carbon fiber composite fuselages in a survivable crash?[J]. *Reinforced Plastics*, 2018, 62(2): 82-88.
- [6] HUANG Yizhou, WANG Zhijin, LIU Gefei. Application of carbon fiber reinforced composite in aerospace[J]. *Journal of Xi'an Aeronautical University*, 2021, 39(5): 44-51.(in Chinese)
- [7] CAO Y, WU Z, SU Y, et al. Aircraft flight characteristics in icing conditions[J]. *Progress in Aerospace Sciences*, 2015, 74: 62-80.
- [8] CAO Y, TAN W, WU Z. Aircraft icing: An ongoing threat to aviation safety[J]. *Aerospace Science and Technology*, 2018, 75: 353-385.
- [9] SHEN Hao, HAN Bingbing, ZHANG Lifan. Research progress of the ice crystal icing in aero-engine[J]. *Journal of Experiments in Fluids Mechanics*, 2020, 34(6): 1-7.(in Chinese)
- [10] MARWITZ J, POLITOVICH M, BERNSTEIN B, et al. Meteorological conditions associated with the ATR72 aircraft accident near Roselawn, Indiana, on 31 October 1994[J]. *Bulletin of the American Meteorological Society*, 1997, 78(1): 41-52.
- [11] HUANG X, TEPYLO N, POMMIER-BUDINGER V, et al. A survey of icephobic coatings and their potential use in a hybrid coating/active ice protection system for aerospace applications[J]. *Progress in Aerospace Sciences*, 2019, 105: 74-97.
- [12] KONG Weiliang. Mechanism and fundamental theory of supercooled water solidification on the abnormal aircraft icing[D]. Shanghai: Shanghai Jiao Tong University, 2015.(in Chinese)
- [13] CHEN Yong, KONG Weiliang, LIU Hong. Challenge of aircraft design under operational conditions of supercooled large water droplet icing[J]. *Acta Aeronautica et Astronautica Sinica*, 2023, 44(1): 626973. (in Chinese)
- [14] JUNG S, TIWARI M K, DOAN N V, et al. Mechanism of supercooled droplet freezing on surfaces[J]. *Nature Communications*, 2012, 3(1): 615.
- [15] ZHANG C, LIU H. Effect of drop size on the impact thermodynamics for supercooled large droplet in aircraft icing[J]. *Physics of Fluids*, 2016, 28(6): 062107.
- [16] LI Yanxin, GU Xin. Development and challenges of supercooled large drop icing research for civil airplane airworthiness certification[J]. *Journal of Civil Aviation University of China*, 2020, 38(4): 48-53.(in Chinese)
- [17] CHEN Shuyue, GUO Xiangdong, WANG Zixu, et al. Preliminary research on size measurement of supercooled large droplet in icing wind tunnel[J]. *Journal of Experiments in Fluids Mechanics*, 2021, 35(3): 22-29. (in Chinese)
- [18] SHUN Jun, XU Dongguang, HAN Zhirong, et al. Hybrid wing design of icing wind tunnel supercooled large droplet icing test[J]. *Acta Aeronautica et Astronautica Sinica*, 2023, 44(1): 627182.(in Chinese)
- [19] WANG Q, LIN X D, LIN Y J, et al. Effects of surface roughness on splashing characteristics of large droplets with digital inline holographic imaging[J]. *Cold Regions Science and Technology*, 2021, 191: 103373.
- [20] KONG W L, WU H C, BIAN P X, et al. A diffusion-enhancing icing theory for the freezing transition of supercooled large water droplet in impact[J]. *International Journal of Heat and Mass Transfer*, 2022, 187: 122471.
- [21] CHANG Shinan, YANG Bo, LENG Mengyao, et al. Study on blend air anti-icing system of aircraft[J]. *Journal of Aerospace Power*, 2017, 32(5): 1025-1034. (in Chinese)
- [22] ZHENG C, DU X, DONG Q, et al. Experimental study of influence of different parameters on flow field structures around an airfoil covered with rough ice[J]. *Journal of Shanghai Jiao Tong University*, 2022, 57(9): 1221-1230.(in Chinese)
- [23] HABIBI H, CHENG L, ZHENG H, et al. A dual de-icing system for wind turbine blades combining high-power ultrasonic guided waves and low frequency forced vibrations[J]. *Renew Energy*, 2015, 83: 859-870.
- [24] LI Zhe, XU Haojun, XUE Yuan, et al. Research on flight safety effect mechanism and protection for aircraft icing[J]. *Flight Dynamics*, 2016, 34(4): 10-14. (in Chinese)
- [25] WANG C, XIAO J, ZENG J, et al. A novel method to prepare a micro flower-like superhydrophobic epoxy resin surface[J]. *Materials Chemistry and Physics*, 2012, 135(1): 10-15.
- [26] WEI W, HUANG R, HUANG C, et al. Cryogenic performances of T700 and T800 carbon fiber epoxy laminates[C]//Proceedings of the Cryogenic Engineering Conference (CEC) / International Cryogenic Materials Conference (ICMC). Tucson, AZ: [s.n.], 2015.
- [27] CAO Yangjing, LI Yuandong, LUO Xiaomei, et al. Effects of casting methods on microstructure, thermal conductivity and mechanical properties of A356 aluminum alloy[J]. *Special Casting & Nonferrous Alloys*, 2021, 41(11): 1424-1430.
- [28] VILLEGAS M, ZHANG Y, ABU J N, et al. Liquid-infused surfaces: A review of theory, design, and applications[J]. *ACS Nano*, 2019, 13(8): 8517-8536.

- [29] KIM A, KIM S, HUH M, et al. Superior anti-icing strategy by combined sustainable liquid repellence and electro/photo-responsive thermogenesis of oil/MWNT composite[J]. *Journal of Materials Science & Technology*, 2020, 49: 106-116.
- [30] WANG X, HUANG X, JI Z, et al. Self-healing ice phobic coating with UV shielding and removability based on biobased epoxy and reversible disulfide bonds[J]. *Polymer*, 2023, 283: 126274.
- [31] ZHANG F, XU D, ZHANG D, et al. A durable and photothermal superhydrophobic coating with entwined CNTs-SiO₂ hybrids for anti-icing applications[J]. *Chemical Engineering Journal*, 2021, 423: 130238.
- [32] WANG L, KONG W, WANG F, et al. Effect of nucleation time on freezing morphology and type of a water droplet impacting onto cold substrate[J]. *International Journal of Heat and Mass Transfer*, 2019, 130: 831-842.
- [33] SUN Mingming, KONG Weiliang, WANG Fuxin, et al. Effect of surface wettability on the law of supercooled large droplet impact and heat transfer[J]. *Journal of Engineering Thermophysics*, 2019, 40(8): 1874-1880. (in Chinese)
- [34] KALIKMANOV V I. Classical nucleation theory, in *Nucleation theory*[M]. [S.l.]: Springer, 2013: 17-41.
- [35] LUBARDA V A, TALKE K A. Analysis of the equilibrium droplet shape based on an ellipsoidal droplet model[J]. *Langmuir*, 2011, 27(17): 10705-10713.
- [36] WU Haocheng, BIAN Peixiang, KONG Weiliang, et al. Nucleation enhancement by energy dissipation with the collision of a supercooled water droplet[J]. *Physics of Fluids*, 2023, 35(1): 013336.
- [37] MCGRAW R, LAVIOLETTE R A. Fluctuations, temperature, and detailed balance in classical nucleation theory[J]. *The Journal of Chemical Physics*, 1995, 102(22): 8983-8994.
- [38] ZHOU L, LIU A, ZHOU L, et al. Facilely fabricated self-lubricated photothermal coating with long-term durability and external replenishing property for anti-icing/deicing[J]. *ACS Applied Materials & Interfaces*, 2022, 14(6): 8537-8548.

Acknowledgement This work was supported by the National Key Laboratory of Advanced Composite Materials (No.KZ42191814).

Authors

The first author Dr. LI Xiaofei received the Ph.D. degree in advanced manufacturing from Shanghai Jiao Tong University, Shanghai, China, in 2024. He carried out research on aircraft icing and anti-icing, and participated in the research of optimized design methods and experimental verification systems for aircraft de-icing systems. His research has focused on aeronautic cutting-edge technology, advanced aeronautic materials and manufacturing technology.

The corresponding authors Prof. HUANG Xiaobin received the Ph.D. degree in materials science from Shanghai Jiao Tong University in 2004. From 2004 to 2014, he has been with College of Chemistry and Chemical Engineering, Shanghai Jiao Tong University, Shanghai, China. From 2014 to present, he has been with School of Aeronautics and Astronautics, Shanghai Jiao Tong University, Shanghai, China. His research has focused on anti-icing functional materials for aircraft, nanomaterials, functional polymers, combustion in extreme environments, and fuel modification and design.

Prof. LIU Hong received the B.S. and M.D. degrees in aero-engine engineering from Nanjing University of Aeronautics and Astronautics, Nanjing, China, in 1994 and 1997, respectively. He received the Ph. D. degree in engineering thermo-physics from Shanghai Jiao Tong University, Shanghai, China, in 2000. From 2000 to 2005, he has been with Department of Engineering Mechanics, Shanghai Jiao Tong University, Shanghai, China. From 2005 to present, he has been with School of Aeronautics and Astronautics, Shanghai Jiao Tong University, Shanghai, China. His research focuses on aircraft design, theoretical research in supersonic aerodynamics, and multidisciplinary design optimization methodologies for aircraft systems.

Author contributions Dr. LI Xiaofei designed the study, conducted the analysis, interpreted the results and wrote the manuscript. Dr. WANG Xiangzhao contributed to materials preparation and data for the analysis of icing characteristics. Dr. JI Zemin contributed to the discussion and background of the study. Prof. HUANG Xiaobin contributed to supervision, project administration and writing. Prof. LIU Hong contributed to methodology and analysis of the study. All authors commented on the manuscript draft and approved the submission.

Competing interests The authors declare no competing interests.

(Production Editor: SUN Jing)

过冷大水滴撞击复材表面结冰特性及防冰研究

李小飞^{1,2}, 王祥昭¹, 吉泽民¹, 黄小彬¹, 刘洪¹

(1. 上海交通大学航空航天学院, 上海 200240, 中国; 2. 中国航空研究院, 北京 100012, 中国)

摘要:碳纤维增强复合材料(Carbon fiber-reinforced composites, CFRCs)的过冷大水滴(Supercooled large droplet, SLD)撞击结冰特性尚未明确,因此难以实现复材飞机结冰防护能力的提升和结冰试航的取证。首先研究不同过冷度、壁面温度和撞击速度对SLD撞击碳纤维增强环氧树脂复合材料表面的结冰特性影响。鉴于CFRCs易结冰的问题,通过引入不同纳米粒子改性的防冰涂层,研究SLD撞击表面改性的碳纤维增强环氧树脂复合材料表面的结冰特性。结果表明经过改性的碳纤维环氧树脂复合材料表面的结冰时间得到极大延迟。其中在水滴温度 -15°C 和壁面温度 -18°C 的条件下,表面疏水改性样品的结冰时间延迟超过1100 ms,比未改性的碳纤维增强环氧树脂复合材料延长了5.4倍。

关键词:飞机结冰;碳纤维增强环氧树脂复合材料;过冷大水滴;疏水改性;结冰防护